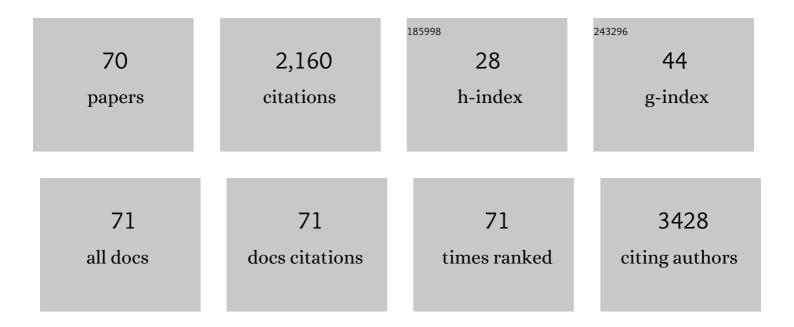
Lian-Cheng Wang

List of Publications by Year in descending order

Source: https://exaly.com/author-pdf/7715719/publications.pdf Version: 2024-02-01



#	Article	IF	CITATIONS
1	WOx/C Heterogeneous Catalyst with Oxygen Vacancies and Deficient Br¶nsted Acid for Epoxidation of 1-Hexene. Catalysis Letters, 2023, 153, 1180-1192.	1.4	3
2	Enhanced hydrogen generation by reverse spillover effects over bicomponent catalysts. Nature Communications, 2022, 13, 118.	5.8	44
3	Ag supported on alumina for the epoxidation of 1-hexene with molecular oxygen: the effect of Ag ⁺ /Ag ⁰ . New Journal of Chemistry, 2022, 46, 4792-4799.	1.4	5
4	Micron-sized iron oxide functionalized with hydrophobic mesoporous sheets for the Ni–Fe battery. Sustainable Energy and Fuels, 2021, 5, 1756-1766.	2.5	2
5	Enhanced Fischer-Tropsch synthesis performances of Fe/h-BN catalysts by Cu and Mn. Catalysis Today, 2020, 343, 91-100.	2.2	10
6	Highly efficient oxidative desulfurization of dibenzothiophene using Ni modified MoO3 catalyst. Applied Catalysis A: General, 2020, 589, 117308.	2.2	73
7	Removal of trace Cr(VI) from aqueous solution by porous activated carbon balls supported by nanoscale zero-valent iron composites. Environmental Science and Pollution Research, 2020, 27, 7015-7024.	2.7	31
8	Amorphous Cr ₂ WO ₆ -Modified WO ₃ Nanowires with a Large Specific Surface Area and Rich Lewis Acid Sites: A Highly Efficient Catalyst for Oxidative Desulfurization. ACS Applied Materials & Interfaces, 2020, 12, 38140-38152.	4.0	42
9	Protection of highly active sites on Cu ₂ O nanocages: an efficient crystalline catalyst for ammonium perchlorate decomposition. CrystEngComm, 2020, 22, 8214-8220.	1.3	8
10	Edge-Activating CO ₂ -Mediated Ethylbenzene Dehydrogenation by a Hierarchical Porous BN Catalyst. ACS Catalysis, 2020, 10, 6697-6706.	5.5	31
11	CoP/RGO-Pd Hybrids with Heterointerfaces as Highly Active Catalysts for Ethanol Electrooxidation. ACS Applied Materials & Interfaces, 2020, 12, 28903-28914.	4.0	16
12	A boron nitride electrode modified with a nanocomposite prepared from an ionic liquid and tungsten disulfide for voltammetric sensing of 4-aminophenol. Mikrochimica Acta, 2019, 186, 614.	2.5	16
13	The role of surface N H groups on the selective hydrogenation of cinnamaldehyde over Co/BN catalysts. Applied Surface Science, 2019, 492, 736-745.	3.1	16
14	Fe containing MoO ₃ nanowires grown along the [110] direction and their fast selective adsorption of quasi-phenothiazine dyes. CrystEngComm, 2019, 21, 5106-5114.	1.3	9
15	N-Doped amorphous MoS _x for the hydrogen evolution reaction. Nanoscale, 2019, 11, 11217-11226.	2.8	43
16	Insight into the Effective Aerobic Oxidative Cross-Esterification of Alcohols over Au/Porous Boron Nitride Catalyst. ACS Applied Materials & Interfaces, 2019, 11, 46678-46687.	4.0	13
17	Anisotropic photogenerated charge separations between different facets of a dodecahedral α-Fe ₂ O ₃ photocatalyst. CrystEngComm, 2019, 21, 6390-6395.	1.3	5
18	Enhanced role of graphitic-N on nitrogen-doped porous carbon ball for direct dehydrogenation of ethylbenzene. Molecular Catalysis, 2019, 462, 61-68.	1.0	32

LIAN-CHENG WANG

#	Article	IF	CITATIONS
19	Micron iron oxide particles with thickness-controllable carbon coating for Ni-Fe battery. Electrochimica Acta, 2019, 299, 800-808.	2.6	20
20	Support Effect of the Fe/BN Catalyst on Fischer–Tropsch Performances: Role of the Surface B–O Defect. Industrial & Engineering Chemistry Research, 2018, 57, 2805-2810.	1.8	24
21	Synergistic enhancement of oxygen reduction reaction with BC3 and graphitic-N in boron- and nitrogen-codoped porous graphene. Journal of Catalysis, 2018, 359, 242-250.	3.1	61
22	Scalable synthesis of quasi-monodispersed BN colloidal nanocrystals by "solvent cutting―and their anti-electrochemical corrosion coating. Chemical Engineering Journal, 2018, 333, 191-199.	6.6	25
23	Design and facile one-step synthesis of FeWO4/Fe2O3 di-modified WO3 with super high photocatalytic activity toward degradation of quasi-phenothiazine dyes. Applied Catalysis B: Environmental, 2018, 221, 169-178.	10.8	72
24	Direct synthesis of 3D hierarchically porous carbon/Sn composites <i>via in situ</i> generated NaCl crystals as templates for potassium-ion batteries anode. Journal of Materials Chemistry A, 2018, 6, 434-442.	5.2	194
25	CoP porous hexagonal nanoplates in situ grown on RGO as active and durable electrocatalyst for hydrogen evolution. Electrochimica Acta, 2018, 284, 534-541.	2.6	29
26	Phosphorus Particles Embedded in Reduced Graphene Oxide Matrix to Enhance Capacity and Rate Capability for Capacitive Potassiumâ€lon Storage. Chemistry - A European Journal, 2018, 24, 13897-13902.	1.7	47
27	Facile Fabrication of BCN Nanosheet-Encapsulated Nano-Iron as Highly Stable Fischer–Tropsch Synthesis Catalyst. ACS Applied Materials & Interfaces, 2017, 9, 14319-14327.	4.0	70
28	Thermal induced BCN nanosheets evolution and its usage as metal-free catalyst in ethylbenzene dehydrogenation. Applied Surface Science, 2017, 422, 574-581.	3.1	34
29	The role of CO2 in dehydrogenation of ethylbenzene over pure α-Fe2O3 catalysts with different facets. Journal of Catalysis, 2017, 345, 104-112.	3.1	28
30	Ultra-thin MoSx film for electrochemical hydrogen production: Correlation between the catalytic activities and electrochemical features. Electrochimica Acta, 2017, 248, 20-28.	2.6	9
31	Iron cation-induced biphase symbiosis of h-WO3/o-WO3·0.33H2O and their crystal phase transition. CrystEngComm, 2017, 19, 3979-3985.	1.3	8
32	Facile synthesis of porous nitrogen-doped holey graphene as an efficient metal-free catalyst for the oxygen reduction reaction. Nano Research, 2017, 10, 305-319.	5.8	57
33	Ultrathin N-rich boron nitride nanosheets supported iron catalyst for Fischer–Tropsch synthesis. RSC Advances, 2016, 6, 38356-38364.	1.7	20
34	Nonspherical hollow α-Fe ₂ O ₃ structures synthesized by stepwise effect of fluoride and phosphate anions. Journal of Materials Chemistry A, 2016, 4, 11000-11008.	5.2	13
35	Formation of Ordered Coronene Clusters in Template Utilizing the Structural Transformation of Hexaphenylbenzene Derivative Networks on Graphite Surface. ACS Nano, 2016, 10, 342-348.	7.3	31
36	Fe–Fe ₃ C/C microspheres as a lightweight microwave absorbent. RSC Advances, 2016, 6, 24820-24826.	1.7	48

LIAN-CHENG WANG

#	Article	IF	CITATIONS
37	Mesoporous Fe/C and Core–Shell Fe–Fe3C@C composites as efficient microwave absorbents. Microporous and Mesoporous Materials, 2015, 211, 97-104.	2.2	54
38	Single-crystal octahedral CoFe2O4 nanoparticles loaded on carbon balls as a lightweight microwave absorbent. Journal of Alloys and Compounds, 2015, 633, 11-17.	2.8	30
39	Restructuring of Co3O4particles from polycrystalline microspheres to single-crystalline polyhedra under the assistance of acetic acid. CrystEngComm, 2015, 17, 1848-1855.	1.3	6
40	NiFe ₂ O ₄ , Fe ₃ O ₄ –Fe _x Ni _y or Fe _x Ni _y loaded porous activated carbon balls as lightweight microwave absorbents. RSC Advances, 2015, 5, 8248-8257.	1.7	20
41	Co3Fe7/C core–shell microspheres as a lightweight microwave absorbent. Materials Chemistry and Physics, 2015, 163, 431-438.	2.0	17
42	Feâ€, Coâ€, and Niâ€Loaded Porous Activated Carbon Balls as Lightweight Microwave Absorbents. ChemPhysChem, 2015, 16, 3458-3467.	1.0	29
43	Hollow CoFe2O4–Co3Fe7 microspheres applied in electromagnetic absorption. Journal of Magnetism and Magnetic Materials, 2015, 377, 259-266.	1.0	39
44	Templated synthesis of highly ordered mesoporous cobalt ferrite and its microwave absorption properties. Chinese Physics B, 2014, 23, 088105.	0.7	25
45	From ultrathin nanosheets, triangular plates to nanocrystals with exposed (102) facets, a morphology and phase transformation of sp2 hybrid BN nanomaterials. RSC Advances, 2014, 4, 14233.	1.7	26
46	CoFe ₂ O ₄ and/or Co ₃ Fe ₇ loaded porous activated carbon balls as a lightweight microwave absorbent. Physical Chemistry Chemical Physics, 2014, 16, 12385-12392.	1.3	82
47	Fabrication of Fe ₃ O ₄ @C core–shell nanotubes and their application as a lightweight microwave absorbent. RSC Advances, 2014, 4, 55738-55744.	1.7	55
48	High-yield synthesis of uniform B, N-rich BN-C x nanoplates in mild temperatures. Journal of Nanoparticle Research, 2014, 16, 1.	0.8	5
49	One pot synthesis of ultrathin boron nitride nanosheet-supported nanoscale zerovalent iron for rapid debromination of polybrominated diphenyl ethers. Journal of Materials Chemistry A, 2013, 1, 6379.	5.2	52
50	Stepwise tuning of the substituent groups from mother BTB ligands to two hexaphenylbenzene based ligands for construction of diverse coordination polymers. CrystEngComm, 2013, 15, 8511.	1.3	9
51	Synthesis of Hollow Boron Nitride Nanoboxes with Ultrathin Walls from Cube-Like LaB ₆ . Journal of Nanoscience and Nanotechnology, 2013, 13, 4634-4638.	0.9	1
52	Corrosion synthesis of boron carbide with pore and hollow structure. International Journal of Refractory Metals and Hard Materials, 2012, 35, 284-287.	1.7	6
53	Facile synthesis of uniform h-BN nanocrystals and their application as a catalyst support towards the selective oxidation of benzyl alcohol. RSC Advances, 2012, 2, 10689.	1.7	20
54	Solid state synthesis of a new ternary nitride MgMoN2 nanosheets and micromeshes. Journal of Materials Chemistry, 2012, 22, 14559.	6.7	25

LIAN-CHENG WANG

#	Article	IF	CITATIONS
55	Synthesis of superconducting sphereâ€like Mo ₂ C nanoparticles in an autoclave. Crystal Research and Technology, 2012, 47, 467-470.	0.6	5
56	High yield synthesis of novel boron nitride submicro-boxes and their photocatalytic application under visible light irradiation. Catalysis Science and Technology, 2011, 1, 1159.	2.1	62
57	Honeycomb-like graphitic ordered macroporous carbon prepared by pyrolysis of ammonium bicarbonate. Materials Research Bulletin, 2011, 46, 1703-1707.	2.7	5
58	Fe3BO5@carbon core–shell urchin-like structures prepared via a one-step co-pyrolysis method. Materials Letters, 2011, 65, 2479-2481.	1.3	1
59	Convenient synthesis and applications of gram scale boron nitride nanosheets. Catalysis Science and Technology, 2011, 1, 1119.	2.1	53
60	Synthesis of MgSiN2 Cuboids by a Solid-state Reaction. Chemistry Letters, 2010, 39, 888-889.	0.7	3
61	A simple pyrolysis route to synthesize leaf-like carbon sheets. Carbon, 2010, 48, 3420-3426.	5.4	20
62	A versatile route for the convenient synthesis of rare-earth and alkaline-earth hexaborides at mild temperatures. CrystEngComm, 2010, 12, 3923.	1.3	43
63	Additiveâ€Assisted Nitridation to Synthesize Si ₃ N ₄ Nanomaterials at a Low Temperature. Journal of the American Ceramic Society, 2009, 92, 517-519.	1.9	12
64	Synthesis and characterization of 3C and 2H-SiC nanocrystals starting from SiO2, C2H5OH and metallic Mg. Journal of Alloys and Compounds, 2009, 484, 341-346.	2.8	24
65	A general route for the convenient synthesis of crystalline hexagonal boron nitride micromesh at mild temperature. Journal of Materials Chemistry, 2009, 19, 1989.	6.7	51
66	Biomimetic Synthesis of Calcium Carbonate Polymorphs Using the Lamellar Lyotropic Liquid Crystalline Systems of Calcium Dodecyl Sulfate. Crystal Growth and Design, 2008, 8, 3560-3565.	1.4	18
67	Convenient Fabrication and Property Investigations of Uniform TiN Hollow Nanocages. Chemistry Letters, 2008, 37, 712-713.	0.7	2
68	Sulfur-assisted Fabrication of Silicon Nitride Nanorods in Autoclaves at 250 °C. Chemistry Letters, 2008, 37, 302-303.	0.7	9
69	Oriented Aggregation and Novel Phase Transformation of Vaterite Controlled by the Synergistic Effect of Calcium Dodecyl Sulfate andn-Pentanol. Journal of Physical Chemistry B, 2006, 110, 23148-23153.	1.2	55
70	Crystallization and Aggregation Behaviors of Calcium Carbonate in the Presence of Poly(vinylpyrrolidone) and Sodium Dodecyl Sulfate. Journal of Physical Chemistry B, 2005, 109, 18342-18347.	1.2	106